Bioelectrochemistry 82 (2011) 1–9

Contents lists available at ScienceDirect

Bioelectrochemistry

journal homepage: www.elsevier.com/locate/bioelechem

Direct electron transfer enhancement of covalently bound tyrosinase to glassy carbon via Woodward's reagent K

Hassan Faridnouri [a], Hedayatollah Ghourchian [a,*], Seddigheh Hashemnia [b]

[a] Institute of Biochemistry and Biophysics, University of Tehran, Tehran 1417614411, Iran
[b] Persian Gulf University, Bushehr 75169, Iran

ARTICLE INFO

Article history:
Received 22 December 2010
Received in revised form 14 April 2011
Accepted 18 April 2011
Available online 22 April 2011

Keywords:
Tyrosinase
Chemical modification
Direct electrochemistry
Woodward's reagent K
Glassy carbon electrode

ABSTRACT

This work describes the reaction mechanism for chemical modification of tyrosinase by Woodward's Reagent K and its covalent attachment to a glassy carbon electrode. The spectrophotometric studies revealed that the modification does not cause a significant structural change to tyrosinase. The direct electrochemistry of modified enzyme was achieved after immobilization on an oxidatively activated glassy carbon electrode. The enzyme film exhibited a pair of well-defined quasi-revesible voltammetric peaks corresponding to the Cu (II)/Cu (I) redox couple located in the active site of tyrosinase. The formal potential of immobilized enzyme was measured to be 90 mV (vs. Ag/AgCl) in phosphate buffer solution at pH 7.0. The charge-transfer coefficient and apparent heterogeneous electron transfer rate constant were estimated to be 0.5 and $0.9 \pm 0.06\ s^{-1}$, respectively. Finally, the electrochemical behavior of the immobilized enzyme in the presence of caffeic acid and L-3,4-dihydroxyphenylalanine as substrates was investigated. The amperometric study of biosensor toward L-3,4-dihydroxyphenylalanine resulted a linear response in the concentration range from 1.66×10^{-6} to 8.5×10^{-5} M with detection limit of 9.0×10^{-5} M and sensitivity of 135 mA μM^{-1} cm^{-2}.

1. Introduction

Protein direct electron transferring is of interest in both theory and practice and can be improved either by electrode or protein modification. In recent years, the direct electron transferring of multi-copper proteins such as laccase, bilirubin oxidase, azurin and ascorbate oxidase have been studied [1–9]. In general, inter-protein electron transfer involves complementary docking sites on each of the redox partners that minimizes the distance between the two redox centers and therefore enhances the electron transfer rate [3]. The establishment of direct electron transfer leads to the construction of reagent-less electrochemical biosensors. By this type of biosensors not only can the generated catalytic current be measured but also the detection of enzyme electron transfer rate becomes feasible. One of the attractive features of enzyme direct electron transferring is the possibility of biosensor design using novel interfacial technologies [10].

In our previous work, we used Woodward's reagent K (WRK) to prepare an active interface for protein immobilization and then, study of protein direct electron transfer[11,12]. WRK is an isoxazolium salt causing rapid and specific modification of carboxylic groups in proteins [13–22]. In the present report we used this technique for covalent attachment of tyrosinase (Tyr) on oxidatively activated glassy carbon (GC) electrode surface. Tyr is a tetramer hydrophilic protein with molecular weight of 120 kDa in which the most charged residues are found on the surface [23]. Since electro-active prosthetic groups of Tyr are deepened inside the structure, it is difficult to directly exchange electrons with the electrode surface. Besides, the adsorption of such a massive molecule on the electrode surface brings about the adsorptive denaturation of the protein. We applied WRK for activation of Tyr carboxylic residues (of aspartate or glutamate) to bind covalently on oxidatively activated GC electrode. We have already used this technique for immobilization of catalase as a huge redox protein however; the resulted voltammogram was irreversible [12]. In the present experience, using this approach not only the stable immobilization of Tyr on GC electrode was obtained but also the direct electron transfer of Tyr and determination of its precise electrochemical properties became possible. There are several reports on direct electron transfer of Tyr in the literature [24–28] however they suffer from some defects. For instance Zhou et al. [28] did not report CV of immobilized Tyr. On the other hand, Sun et al. [25], Mohammadi et al. [24] and Yaropolov et al. [26] did not report some kinetic parameters of the immobilized Tyr such as heterogeneous electron transfer rate constant. Also, Ye et al. [27] investigated the direct electrochemistry of Tyr at silver in the solution. To our knowledge the direct electrochemistry of chemically modified Tyr which covalently attached on an oxidatively activated GC electrode has not been reported yet.

* Corresponding author. Tel.: +98 21 66408920; fax: +98 21 66404680.
E-mail addresses: faridnouri@ibb.ut.ac.ir (H. Faridnouri), hadi@ibb.ut.ac.ir (H. Ghourchian), hashemnia@pgu.ac.ir (S. Hashemnia).

1567-5394/$ – see front matter © 2011 Elsevier B.V. All rights reserved.
doi:10.1016/j.bioelechem.2011.04.004

2. Experimental section

2.1. Materials

All chemicals were of analytical grade and used without further purification. Mushroom Tyr (EC 1.14.18.1, 5370 U/mg, Cat No. T-3824), perfluorinated ion-exchange resins (Nafion, 5% in ethanol), L-3,4-dihydroxyphenylalanine (L-DOPA) and bovine serum albumins (BSA) were purchased from Sigma. 2-Ethyl-5-phenylisoxazolium-3-sulfonate (Woodward's reagent K) was obtained from Aldrich, 1-anilino-8-naphthalenesulfonate (ANS), caffeic acid and phosphate buffer salts were obtained from Merck (Germany). All experiments were carried out at 25 °C. All samples were prepared in 0.1 M phosphate buffer solution (PBS), pH 7.0 using doubly distilled water.

2.2. Spectroscopic measurements

A Shimadzu UV-3100 spectrophotometer equipped with a water bath (±0.5 °C) was used for determination of Tyr concentration and assay. The spectra of native and WRK-modified Tyr were recorded at the wavelength range of 200–600 nm. The concentration of Tyr stock solution in PBS (0.1 M, pH 7.0) was determined at 280 nm, using Tyr molar extinction coefficient ($\varepsilon_{280} = 2.27 \times 10^{-5}\ M^{-1}\ cm^{-2}$). Kinetic assay of catecholase activity of Tyr was carried out in a conventional quartz cell through depletion of caffeic acid for 2 min at 311 nm and 25 ± 0.1 °C, while the enzyme concentration was 11.8 μM (40 U/ml) [29].

For the secondary structural analysis a circular dichroism (CD) spectrometer model 215 (Aviv Instruments INC, USA) was used. The far-UV CD spectra of the native or modified Tyr (0.4 mg/ml) in PBS were recorded at the wavelength range of 190–260 nm with a spectral resolution of 1 nm at 25 °C. The scan speed, response time and bandwidth were 20 nm min^{-1}, 0.33 s and 1 nm, respectively. A quartz cell with an optical path of 1 mm was used. The far-UV CD spectra were analyzed for the secondary structural elements of the native and modified Tyr using CDNN program, version 2 (http://bioinformatik.biochemtech.uni-halle.de/cdnn).

Fluorescence measurement was carried out using a Hitachi Fluorescence Spectrophotometer model MPF-4 (Japan). Tyr (0.4 mg/ml) was incubated with 24 μM ANS in PBS for 15 min. The sample was exited at 380 nm and the fluorescence emission was recorded from 400 to 650 nm at 25 °C.

2.3. Electrochemical measurements

The electrochemical measurements were carried out using a 263A potentiostat/galvanostat (EG&G, USA) equipped with a PowerSuite software package and a GPIB interface. A conventional three-electrode cell consisting of a GC electrode (diameter 0.2 mm, from Azar Electrode, Uromia, Iran), a silver/silver chloride reference electrode (3 M KCl solution, from Metrohm), and a platinum rod counter electrode were used as working, reference and counter electrode, respectively at 25 ± 1 °C.

2.4. Electron microscopy

Scanning electron microscopy (SEM) images of the immobilized proteins on GC electrode were obtained with a Ziess EM 902A Scanning Electron Microscope (Germany). For each SEM image, the electrode tip was detached from the electrode body and coated with a thin layer of gold.

2.5. Chemical modification of Tyr

The modification of exposed carboxylate groups of Tyr was carried out selectively using WRK. Different concentration of WRK (0.5, 1, 5 and 10 mM) was added to the different concentrations of native Tyr at room temperature and incubated for 30 min. Using the procedure reported by Sinha and Brewer [21], the number of carboxylate groups modified by WRK is proportional to the increase of absorbance at 340 nm ($\varepsilon_{340} = 7000\ M^{-1}\ cm^{-1}$). The stability of WRK is pH dependent and rapidly gets destroyed at pH values above 3.0 [19]. For this reason, we used a large excess of WRK over the enzyme in order to compensate the instability of the reagent at pH 7.0. Then, to remove the excess WRK the reaction mixtures were dialysed for 72 h at 4.0 °C. Thereafter, the modified Tyr (WRK–Tyr) was applied for spectrophotometric, electrochemical and electron microscopic studies.

2.6. The working electrode preparation

Prior to each experiment, the working electrode was cleaned using the following method. First, it was polished with 0.6 and 0.03 μm alumina suspension, respectively. Then it was rubbed on a filter paper and rinsed with deionized water and then, sonicated in a beaker containing a 1:1 (v/v) mixture of deionized water/ethanol for 10 min using a Techno-Gaz ultrasonic cleaner (Italy). The electrode was oxidatively activated by applying the potential of +1.5 V for 2 min in PBS (0.1 M, pH 7.0). Thereafter, 10 μl of WRK–Tyr was dropped on the oxidatively activated electrode and then, the enzyme-coated electrode was covered by 2 μl of 5% Nafion to obtain the Nafion/WRK–Tyr/GC electrode. Finally, the electrode was allowed to dry at room temperature and then the prepared electrode was stored at 4.0 °C. In a parallel experiment, BSA was modified in the same way and used as control. For electrochemical measurements, the test solution was first carefully degassed using highly purred nitrogen gas and then maintained under a nitrogen flow during the voltammetric experiment.

For amperometric experiment a rotating disc electrode with the rotation speed of 500 rpm was used under the constant potential of −200 mV (vs. Ag/AgCl, 3 M KCl) in an electrochemical cell containing 4 ml of phosphate buffer 0.1 M, pH 7.0. At first the background current was allowed to reach to a steady-state then the aliquots of L-DOPA solutions were added to the electrochemical cell.

3. Results and discussion

3.1. Mechanism of Tyr immobilization

The reaction of WRK with a carboxylate anion and immobilization mechanism of modified Tyr is demonstrated in Scheme 1. Irreversible formation of a ketoketenimine is the first step of the reaction, which then reacts with a carboxylate group to give an enol ester, showing an absorption peak at 345 nm [22]. This reaction is initiated by the abstraction of a proton from the reagent by a base or water, causing an immediate rearrangement to highly reactive ketoketenimine intermediate, which then rapidly reacts with a carboxylate group on the protein to form an enol ester. Finally, enol ester bond may further react with appropriate nucleophiles [18,19]. In this study we used an electrochemically activated GC electrode as the appropriate nucleophiles. During the electrochemical treatment, the oxidized functional groups of alcohol or phenol appeared on the electrode surface [30,31]. These functional groups, as nucleophiles, react with enol ester derivative of Tyr. By this mechanism the enzyme covalently bound to GC electrode surface.

3.2. Morphological characterization of the Nafion/WRK–Tyr film

Fig. 1 represents the morphology of Nafion (A), Nafion/Tyr (B) and Nafion/WRK–Tyr (C) on pretreated GC electrode surface. Nafion is formed in micro phase separated morphology of spherical shaped in which the hydrophilic regions containing sulfonate groups are

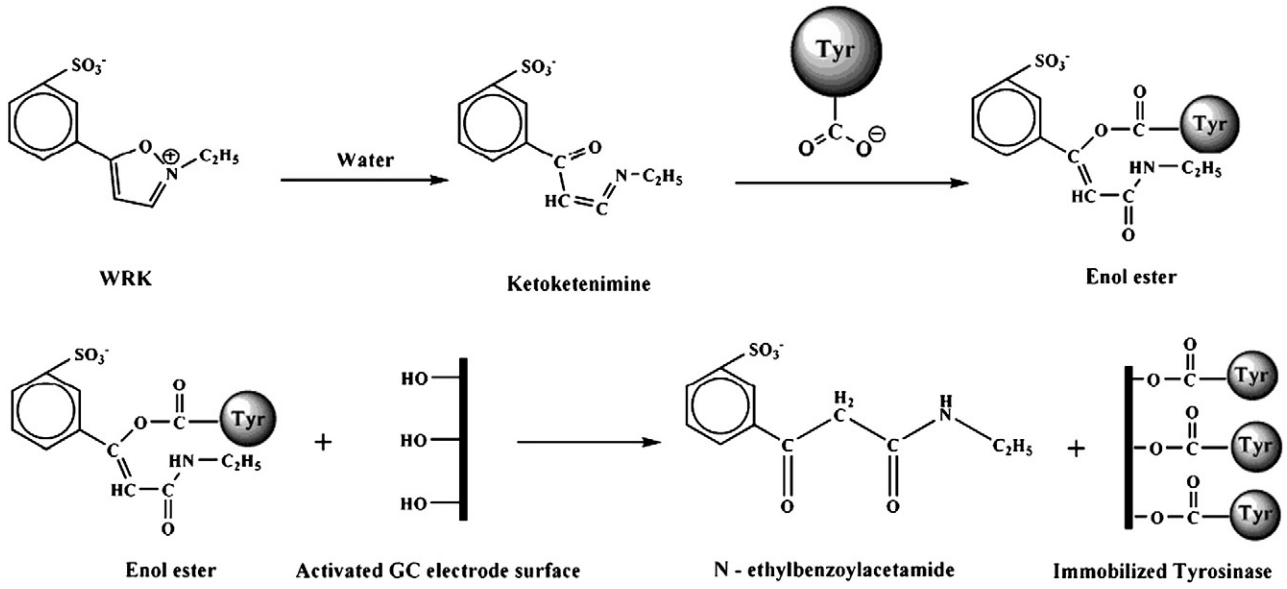

Scheme 1. The reaction mechanism of enzyme chemical modification and its covalent attachment to activated GC electrode.

embedded in hydrophobic regions composed by a perfluorinated bone [31]. While, co-deposition of Tyr and Nafion generated a non-uniform membrane on which globular spots of protein emerge over a smooth polymer coating. Therefore, it seems that the high molecular weight Tyr is covered by the polymeric net. Most certainly, the Nafion/WRK–Tyr film on GC electrode produces a high heterogenic membrane, where the microstructure of polymer has distorted and effectively acts as a protein retentive agent. The composite membrane of Nafion/WRK–Tyr film (Fig. 1C) exhibits much more bulbous spots in comparison with Nafion/Tyr film (Fig. 1B). This indicates that the modified Tyr is absorbed on activated GC electrode much more than native enzyme.

3.3. Spectrophotometric properties

As shown in Fig. 2A, comparison of the UV–Vis spectra of the native (blue line) and modified enzyme (pink, red and green lines) indicates that owing to the modification of Tyr a new absorption peak was appeared at around 345 nm. This peak could be a sign for the formation of a stable enol ester bond due to the modification of Tyr carboxylate residues (aspartate or glutamate) via WRK [21,32–34]. Also the significant intensity at 280 nm (Fig. 2A, spectrum green) shows that Tyr modification is optimized at 5 mM WRK. At over this concentration, WRK leads to the enzyme denaturation (data not shown). Although the attachment of WRK to Tyr carboxyl residues adjoins the new functional groups containing delocalized electron which intern rises up the absorbance intensity, but no significant shift was observed at 280 nm. This confirms that the enzyme active site remained unchanged. Of course, addition of the WRK may cause a little conformational change in the modified Tyr, but the enzyme assay revealed that the activity was not drastically changed (results not shown). So, 5 mM was applied as the optimum concentration of WRK for enzyme modification in the next experiments.

The solvent exposure of non-polar clusters on the native and modified Tyr was studied by ANS binding. This fluorescent probe binds to non-polar clusters on protein surface [35]. Fig. 2B shows the ANS fluorescence spectra bound to the native and modified Tyr. The significant fluorescence intensity at about 521 nm indicates the hydrophobic interaction between ANS and the exposed hydrophobic patches on the native Tyr [36]. However, the fluorescence properties of ANS interacting with modified Tyr show a significant quenching of ANS fluorescence intensity without shift of emission at λ_{max}. This indicates that in the attached WRK the effect of polar groups dominate to the aromatic patches; therefore, the exposed hydrophobic patches were reduced due to Tyr modification.

In order to determine the effect of chemical modification of carboxylic residues on the protein structural properties at the secondary folding level, CD spectroscopy was used. Fig. 2C shows that the far-UV CD spectra of the native and modified Tyr at negative extremes of 212 and 220 nm are almost similar. The contents of α-helix, β-sheet, β-turn and random coil in each spectrum were analyzed using the CDNN program version 2, which was represented in Table 1. Regarding the 5–10% error in software analysis, the modification of enzyme by WRK caused no significant conformational change in Tyr secondary structure.

3.4. Electrochemical features of Nafion/WRK–Tyr film

Due to the adsorptive denaturation of large proteins such as Tyr on bare electrode, it is impossible for protein to directly exchange electrons with the electrode surface [37–39]. As shown in the previous section, the secondary structure of the modified enzyme did not significantly change while, its hydrophobic patches was decreased. On the other hand, the oxidative treatment of the electrode causes an increase in hydrophilic groups on the electrode surface [31]. The modification of Tyr and oxidative treatment of GC electrode decrease the hydrophobic interactions between the enzyme and electrode surface. On the contrary, as we will consider in the next sections, the formation of the enol ester bound between enzyme and oxidized functional groups of electrode not only keeps the enzyme in its native form but also facilitates the enzyme electron transfer process. Therefore, this immobilization method prevents the adsorptive denaturation of the protein.

3.4.1. Cyclic voltammetry of WRK–Tyr

Cyclic voltammetry is an effective method for probing the feature of surface-modified electrode and testing the kinetic barrier of the interface. Therefore, the electrochemical behavior of native and

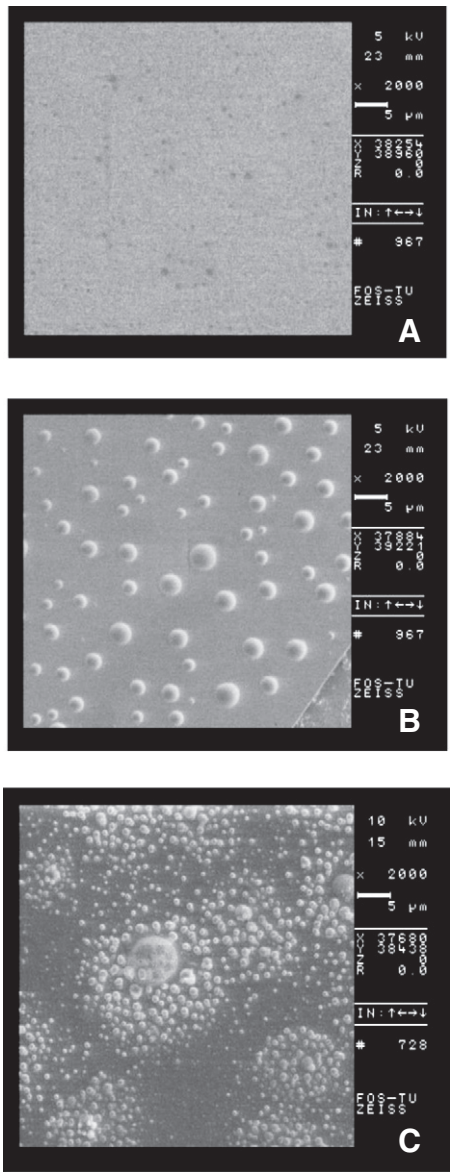

Fig. 1. SEM images of different modified GC electrode surfaces. (A) Nafion/GC, (B) Nafion/Tyr/GC and (C) Nafion/WRK–Tyr/GC at ×2000.

Table 1
Percentage of the secondary structure components for native and modified Tyr.

Percentage secondary structure	Enzyme type	
	Native Tyr	Modified Tyr
Helix	31.9	30.9
Antiparallel	8.8	9.2
Parallel	9.3	9.6
Beta turn	16.9	17.2
Random coil	34.6	35.1
Total sum	101.6	102

The data were extracted from Fig. 2C and analyzed based on cdnn program version 2.

modified Tyr was studied by cyclic voltammetry. At first the electrochemistry of native and modified Tyr in buffer solution was examined. Tyr, WRK or WRK–Tyr did not show voltammetric response in solution (data not shown). Also drop coating of the native Tyr on the naked GC electrode exhibited no distinguished redox peak (Fig. 3, blue line). The Nafion/WRK–Tyr film on activated GC electrode showed a pair of well-defined quasi-reversible and nearly symmetrical peaks at about −20 and +200 mV vs Ag/AgCl at scan rate of 100 mV s^{-1} (Fig. 3, purple line). The formal potential ($E^{\circ\prime}$) of Nafion/WRK–Tyr/GC was determined to be 90 mV vs. Ag/AgCl (287 mV vs. NHE). However, this value is in the range of the $E^{\circ\prime}$ values reported for Tyr from different sources and different methods of immobilization (120 to 600 mV vs. NHE) [40]. The ratio of the cathodic/anodic current was found to be close to 1. Also, in order to control the covalent bound of the WRK–Tyr on activated GC electrode, the CV of WRK–Tyr/GC electrode, without Nafion coating, in the same condition was studied (Fig. 3 green line). As seen, an electrochemical behavior similar to that of Nafion/WRK–Tyr was observed while the peaks height was relatively reduced and $E^{\circ\prime}$ decreased to 75 mV. This confirms an intimate electronic communication between immobilized WRK–Tyr and GC electrode surface which is in agreement with the proposed immobilization mechanism. On the other hand, positive shift (+15 mV) of $E^{\circ\prime}$ in Nafion/WRK–Tyr/GC relative to WRK–Tyr/GC indicated an improvement in the electron transfer ability and facilitating the electrode reaction. The Nafion coating causes relatively more reversible peaks, because based on the Equation: $\Delta G = -nF\Delta E^{\circ\prime}$, the positive shift of $E^{\circ\prime}$ makes the $\Delta G < 0$.

Difference between the peaks intensity of WRK–Tyr/GC and Nafion/WRK–Tyr/GC brought us to this conclusion that two types of Tyr molecules play role in electronic communication with GC electrode. First, those molecules which covalently bond on the

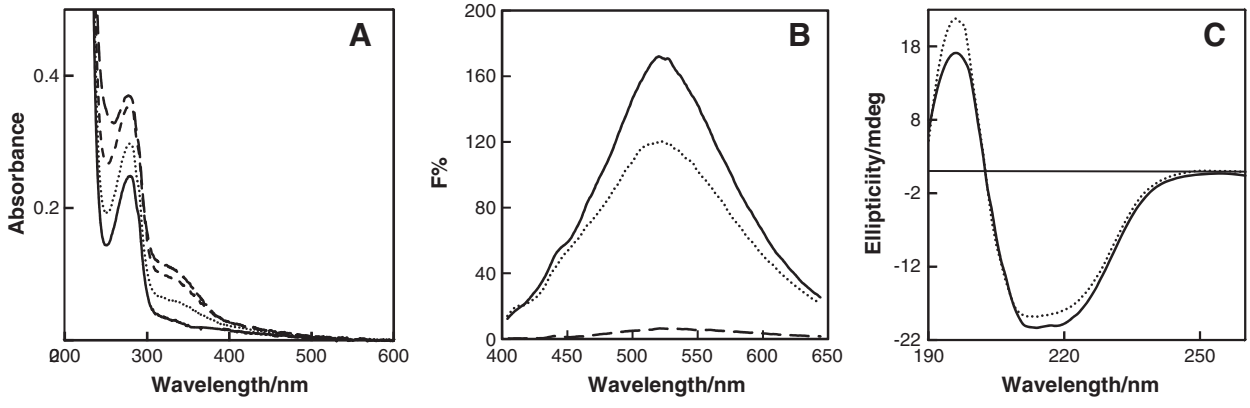

Fig. 2. (A) UV–Vis spectra of the native and modified Tyr. The lines from down to up show the spectrum of native Tyr and Tyr modified by different concentrations of WRK: 0.5, 1, and 5 mM, respectively. (B) ANS fluorescence spectra of the native and modified Tyr. The dashed line shows the spectrum of free ANS. The solid and dotted lines represent ANS fluorescence spectra bound to the either native or modified Tyr (0.4 mg/ml) respectively. The excitation wavelength was 380 nm and the slit width was10 nm. (C) The far-UV CD spectra of native (solid line) and modified (dotted line) Tyr. All experiments were performed in 0.1 M phosphate buffer (pH 7.0) at 25 °C.

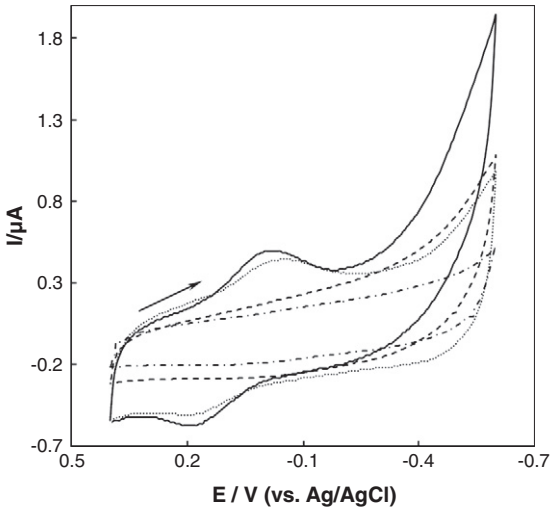

Fig. 3. CVs of Nafion/Tyr/GC, Nafion/WRK-BSA/GC, WRK -Tyr/GC and Nafion/WRK -Tyr/GC electrodes, from inner to outer, respectively. Scan rate was 100 mV s^{-1}.

electrode surface through the mechanism explained in Scheme 1. Second, are those Tyr molecules which adsorbed on Nafion coating. As reported previously, Nafion may offer a biocompatible microenvironment to confine bio-macromolecules at its ionic cluster region (30–50 nm), based on polar/non-polar microphase separation in a hydrated ionomer [41]. So, it seems that Nafion preserve the adsorbed Tyr molecules in the vicinity of the covalently bounded Tyr on GC electrode and consequently amplify the signal (Fig. 3, purple line). In addition, this process leads to conservation of the enzyme layer on electrode surface for a longer time in comparison to the WRK–Tyr/GC electrode without Nafion coating (data not shown).

In order to demonstrate the performance of immobilization method in direct electron transfer of Tyr, the method was applied for a non redox protein (BSA) modified with WRK, too. Then the cyclic voltammogram (CV) of Nafion/WRK-BSA film on GC electrode was studied as control (Fig. 3, dotted line). Essentially, no voltammetric response was observed for the modified BSA film. This experimental result confirms that the voltammetric response in Fig. 3 (solid line) is related to Tyr redox couple of Cu(II)/Cu(I). Thus, the comparison of CVs at different conditions revealed that chemical modification along with immobilization of the enzyme provides a favorable condition for the enzyme to exchange electrons with the underlying GC electrode.

To obtain the kinetic parameters of the immobilized enzyme on the activated GC electrode, the scan rate effect was investigated (Fig. 4A). Both the anodic and cathodic peak currents (I_{pa} and I_{pc}) were linearly increased with scan rate change in the range from 5 to 1000 mVs^{-1} (Fig. 4B). This suggests that the electrode reaction corresponds to a typical surface-controlled electrochemical process as expected for immobilized systems [42]. The regression equation for cathodic and anodic peak current was $I_{pc} = -4.44\nu - 117.5$, $R = 0.9989$ and $I_{pa} = 4.017\nu + 84.717$, $R = 0.9993$, respectively.

The slope obtained for linear regression of log I_p vs. log ν (Fig. 4C) was 0.92 ($R = 0.9993$). This slope is close to the value of 1, as expected for the thin layer electrochemical behavior [43].

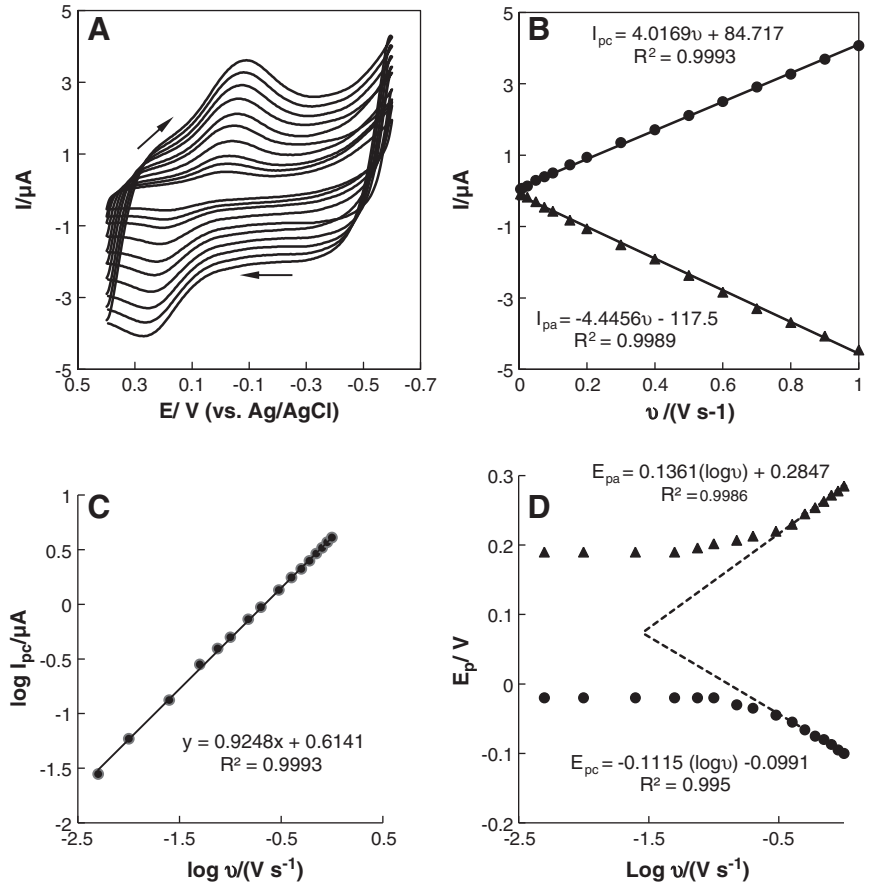

Fig. 4. (A) CVs of Nafion/WRK–Tyr/GC at different scan rates from inside to outside: 100, 150, 200, 300, 400, 500, 600, 700, 800 and 900 mV s^{-1}, respectively. (B) Dependence of peak currents on scan rate, (C) Epc vs. log ν and (D) Log Ipc vs. log ν.

The amount of immobilized enzyme on the electrode surface can be estimated from integration of peak currents in the CVs according to Eq. (1)[44]:

$$I_p = n^2F^2\nu A\Gamma / 4RT \quad (1)$$

where, Γ (mol cm^{-2}) is the surface coverage of adsorbed WRK–Tyr, A (cm^2) is the real electrode surface area, and n is the number of electron transferred in the rate determining reaction and the other symbols have their usual meanings. Assuming a two-electron transfer, the amount of protein molecules is estimated to be 3.4×10^{-11} mol cm^{-2}. It indicated that a thin layer of WRK–Tyr molecules takes the electrode reaction which is in agreement with result of Log I_{pc} vs. Log ν.

The kinetic parameters of charge-transfer coefficient (α) and heterogeneous transfer rate constant (k_s) are estimated using Eq. (2), for nΔEp>0.200 V [45].

$$logk_s = \alpha\ log(1-\alpha) + (1-\alpha)\ log\alpha - log\frac{RT}{nF\nu} - \frac{\alpha(1-\alpha)nF\Delta E_p}{2.3RT} \quad (2)$$

Here, ν is the scan rate; n is the number of transferred electrons of the rate determining reaction and ΔE_p is the difference between cathodic (E_{pc}) and anodic (E_{pa}) peak potential. The other symbols have their usual meanings.

A graph of the peak potential vs. the logarithm of the scan rate yields a straight line at scan rates >300 mVs^{-1} (Fig. 4D). An average value of α = 0.5 was calculated using the slopes of −2.3RT/αnF and 2.3RT/(1 − α) nF for the cathodic and anodic peak, respectively. Afterwards, an average value of 0.9 ± 0.06 s^{-1} was obtained for k_s which in comparison with the values obtained by the silver electrode (0.03 s^{-1}) [27] is faster.

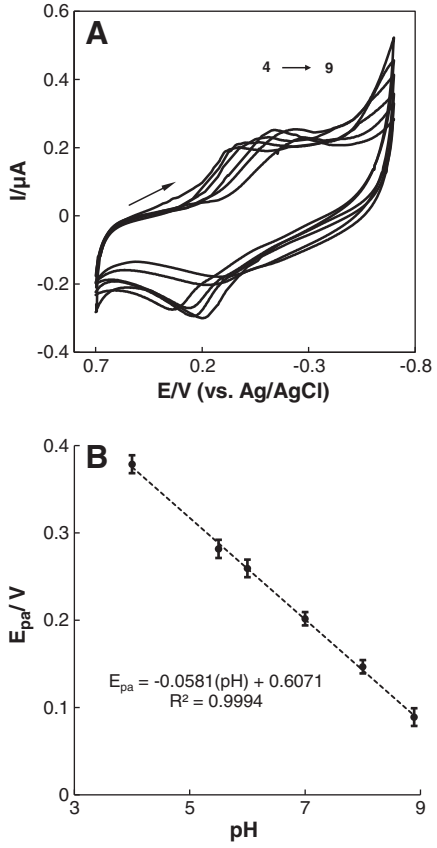

Fig. 5. (A) CVs of Nafion/WRK–Tyr/GC at pH 4, 5.5, 6, 7, 8 and 9 from left to right, respectively. (B) The plot of Ea vs. pH. The scan rate was 0.1 V s^{-1}. All experiments were performed in 0.1 M PBS at 25°.

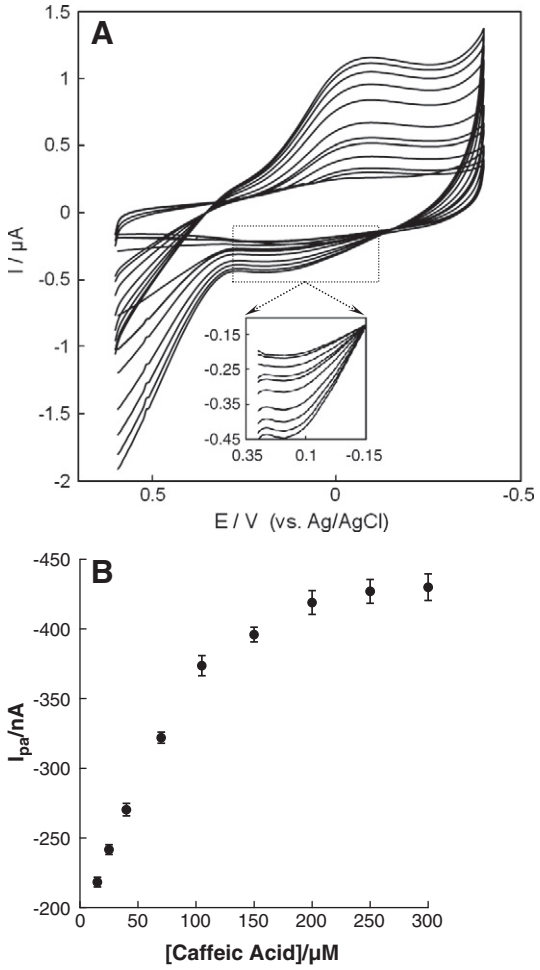

Fig. 6. (A) CVs of Nafion/WRK–Tyr/GC in the presence of different concentrations of caffeic acid, from inside to outside: 0, 15, 25, 40, 70, 100, 150, 200, 250 and 300 μM. (B) Increasing trend of Tyr anodic peak current. The experiments were carried out in 0.1 M air saturated PBS, pH 7.0 at the scan rate of 100 mV s^{-1}.

3.4.2. pH effect

Fig. 5A shows the CVs obtained by Nafion/WRK–Tyr/GC electrode at different pH from 4.0 to 9.0. The pH changes cause a negative shift in E_a of WRK–Tyr. This indicates that hydrogen ion is involved in the redox process, and therefore, the solution pH is effective in the active site conformation change and ionization of some amino acids residues by which catalytic action of Tyr is performed. The slope of the E_a vs. pH is 58.1 mV pH^{-1} (Fig. 5B), which is close to the theoretical value of 59.0 mV pH^{-1} for a two-proton coupled with two-electron redox reaction process [44]. The pH value does also affect on the redox peak currents of WRK–Tyr. Obviously, the maximum peak current was observed at an optimal pH range between 6.0 and 7.0.

3.4.3. Catalytic activity of immobilized Tyr

The catalytic activity of immobilized Tyr (Nafion/WRK–Tyr/GC electrode) on caffeic acid was assessed by cyclic voltammetry (Fig. 6A). Based on Solomon et al. [45], the resting state of the enzyme is mainly in the oxidized form [Tyr–Cu(II)] which can interact with diphenolic compounds such as caffeic acid. The products of this catalytic reaction is the oxidized form of caffeic acid (*o*-quinone) and the reduced form of the enzyme [Tyr–Cu(I)]. Therefore, by increasing the amounts of caffeic acid, the concentration of [Tyr–Cu(I)] is also increased. This, in turn, causes the greater anodic peak current

(Scheme 2A) as seen in the inset of Fig. 6A. In the other hand, as shown in Scheme 2B, the produced *o*-quinone can be changed into caffeic acid at about −100 mV. This causes the greater cathodic peak current as seen in Fig. 6A. Calibration curve of caffeic acid based on changes of the anodic peak current with regression equation of I_{pa} (nA) = −1.709 [caffeic acid] (μM) − 198, $R^2 = 0.995$ was presented in Fig. 6B.

Comparison of the CVs of Tyr in the absence and presence of caffeic acid showed that in the presence of caffeic acid the cathodic peak was shifted to negative potential while no shift was observed in anodic peak potential. It was expected that in the presence of caffeic acid the cathodic peak current of enzyme decreases (at about −20 mV) due to Tyr–Cu(II) consumption. In contrary, not only this peak was increased but also it was shifted to −100 mV. Since the concentration of *o*-quinone is much higher than that of the immobilized Tyr, the cathodic peak of *o*-quinone overcomes the reduction peak of Tyr. Therefore, the reduction peak current of the enzyme at about −20 mV was covered by strong cathodic peak of *o*-quinone at −100 mV.

These results indicate that the catalytic activity of Tyr is reserved in its modified or immobilized form.

Finally the electrochemical biosensing of L-DOPA was performed under air saturated condition. Fig. 7A illustrates the typical current–time plot of the biosensor at the applied potential of −200 mV in PBS (0.1 M, pH 7.0). By addition of subsequent aliquots of L-DOPA into the buffer solution under constant stirring, the stepwise increase of the reduction current was detected. The response time, as the period during which 95% of steady-state response is achieved, was less than 10 s. Such a fast response could be due to the very low thickness of Nafion-enzyme layer on the electrode surface which makes the substrate diffusion easier.

As shown in Fig. 7B, the biosensor response toward L-DOPA was linear in the concentration range from 1.66×10^{-6} to 8.5×10^{-5} M with a regression equation of: I (nA) = 4.26 [L-DOPA] (μmol L^{-1}) + 0.032, (R = 0.9977). At signal-to-noise ratio of 3, the detection limit and sensitivity were calculated to be 9.0×10^{-5} M and 135 mA μM^{-1} cm^{-2}, respectively.

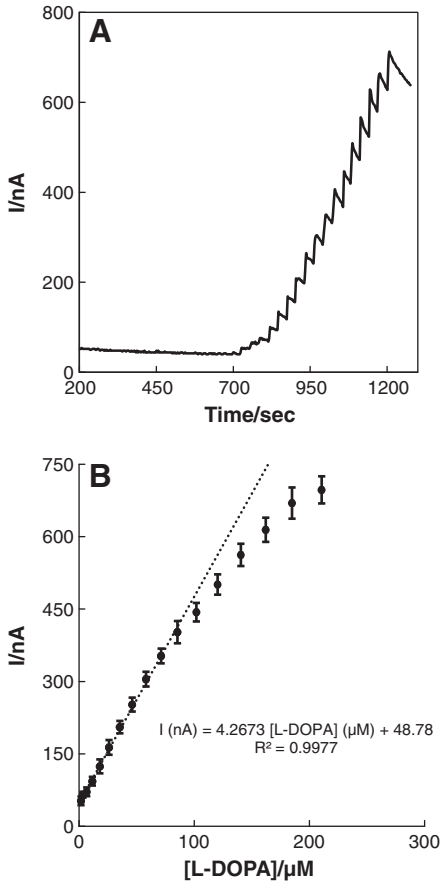

Fig. 7. (A) Calibration curve of the Nafion/WRK–Tyr/GC biosensor toward L-DOPA. (B) Dynamic response of biosensor to successive addition of L-DOPA at the applied potential of −200 mV (vs. Ag/AgCl), in 0.1 M PBS (pH 7.0).

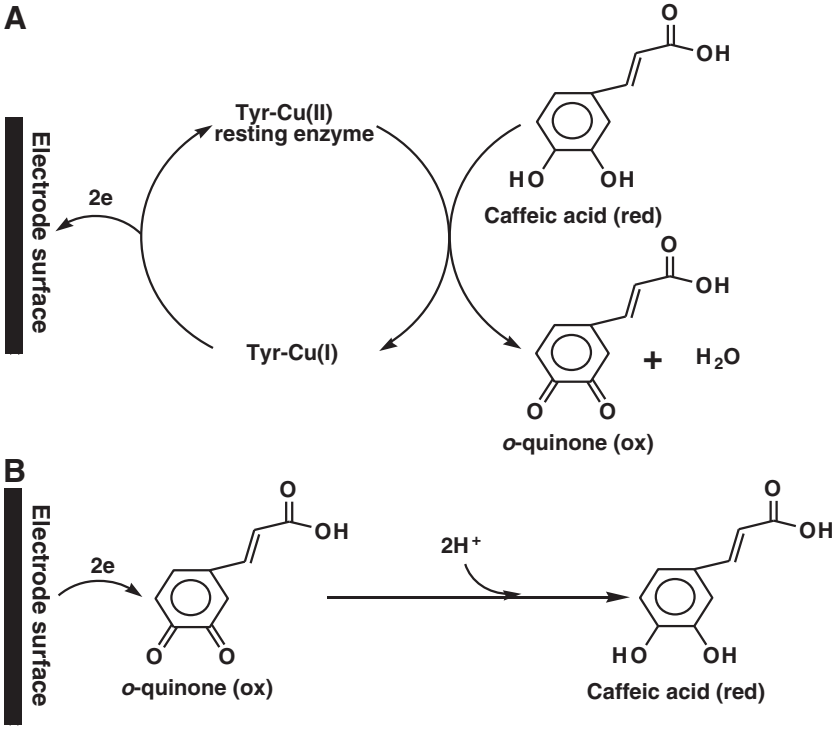

Scheme 2. Representation of electron transfer between Tyr and GC electrode during the diphenolase activity of immobilized Tyr. A: anodic reaction and B: cathodic reaction.

3.4.4. Reproducibility and stability of the Nafion/WRK–Tyr film electrode

Operational and storage stability of biosensors are two important characteristics for the evaluation of the device. In a cyclic voltammetric test, the operational stability of WRK–Tyr based biosensor was assessed. More than 95% of the WRK–Tyr peak height retained after 50 cycles at the scan rate of 100 mV s^{-1} while the peak potential remained unchanged. To control the storage stability, the electrode was stored at 4.0 °C for 2 weeks and no change in the CVs was observed. It seems that this stability can be attributed to two factors. The covalent attachment of WRK–Tyr to the oxidatively activated GC electrode prevents enzyme detaching from the electrode surface. Also nafion polymer protects Tyr from quinones formed during the Tyr-catalysed reaction. Quinones are capable of reacting with the free amino groups of the enzyme and inactivating the enzyme [46].

4. Conclusion

The presented mechanism for Tyr immobilization revealed that the chemically modified enzyme is tightly attached to GC electrode. This not only led to the achievement of enzyme direct electrochemistry but also resulted in development of a biosensor for caffeic acid and L-DOPA detection. Comparison of the characteristics of native and modified enzymes such as catalytic activity and secondary structure components revealed that the modification does not cause a distinguished structural change to Tyr. Due to the covalently attachment of enzyme to the electrode surface, a satisfactory storage and operational stability was obtained for the immobilized enzyme. It seems that using this reaction mechanism the direct electrochemistry of other copper containing enzymes can also be achieved. The feasibility of this supposition and also optimization of the experimental parameters for amperometric detection of phenolic substrates in real sample is currently under investigation in our laboratory.

Acknowledgement

The financially supports of the Research Council of the University of Tehran and Iran National Science Foundation (INSF) are gratefully acknowledged. The cooperation of the electron microscope staff at the Science College of Tehran University is also acknowledged.

References

[1] W. Zheng, Q.F. Li, L. Su, Y.M. Yan, J. Zhang, L.Q. Mao, Direct electrochemistry of multi-copper oxidases at carbon nanotubes noncovalently functionalized with cellulose derivatives, Electroanalysis 18 (2006) 587–594.
[2] M. Tominaga, M. Otani, M. Kishikawa, I. Taniguchi, UV–ozone treatments improved carbon black surface for direct electron-transfer reactions with bilirubin oxidase under aerobic conditions, Chem. Lett. 35 (2006) 1174–1175.
[3] S. Shleev, J. Tkac, A. Christenson, T. Ruzgas, A.I. Yaropolov, J.W. Whittaker, L. Gorton, Direct electron transfer between copper-containing proteins and electrodes, Biosens. Bioelectron. 20 (2005) 2517–2554.
[4] S. Shleev, A. Jarosz-Wilkolazka, A. Khalunina, O. Morozova, A. Yaropolov, T. Ruzgas, L. Gorton, Direct electron transfer reactions of laccases from different origins on carbon electrodes, Bioelectrochemistry 67 (2005) 115–124.
[5] T. Sakurai, Cyclic voltammetry of cucumber ascorbate oxidase, Bioelectrochemistry (1996) 481–482.
[6] M. Pita, S. Shleev, T. Ruzgas, V.M. Fernandez, A.I. Yaropolov, L. Gorton, Direct heterogeneous electron transfer reactions of fungal laccases at bare and thiol-modified gold electrodes, Electrochemistry Communications 8 (2006) 747–753.
[7] J.P. McEvoy, J.S. Foord, Direct electrochemistry of blue copper proteins at boron-doped diamond electrodes, Electrochimica Acta 50 (2005) 2933–2941.
[8] B.D. Fleming, J. Zhang, D. Elton, A.M. Bond, Detailed analysis of the electron-transfer properties of azurin adsorbed on graphite electrodes using dc and large-amplitude Fourier transformed ac voltammetry, Anal. Chem. 79 (2007) 6515–6526.
[9] P.D. Barker, K. Digleria, H.A.O. Hill, V.J. Lowe, Electron-transfer reactions of metalloproteins at peptide-modified gold electrodes, Eur. J. Biochem. 190 (1990) 171–175.
[10] L. Gorton, A. Lindgren, T. Larsson, F.D. Munteanu, T. Ruzgas, I. Gazaryan, Direct electron transfer between heme-containing enzymes and electrodes as basis for third generation biosensors, Anal. Chim. Acta 400 (1999) 91–108.
[11] S. Hashemnia, A.A. Moosavi-Movahedi, H. Ghourchian, F. Ahmad, G.H. Hakimelahi, A.A. Saboury, Diminishing of aggregation for bovine liver catalase through acidic residues modification, Int. J. Biol. Macromol. 40 (2006) 47–53.
[12] S. Hashemnia, H. Ghourchian, A.A. Moosavi-Movahedi, H. Faridnouri, Direct electrochemistry of chemically modified catalase immobilized on an oxidatively activated glassy carbon electrode, Journal of Applied Electrochemistry 39 (2009) 7–14.
[13] J.L. Arana, R.H. Vallejos, Two different types of essential carboxyl groups in chloroplast coupling factor, FEBS Lett. 123 (1981) 103–106.
[14] A.J. Brake, B.H. Weber, Evidence for an essential carboxyl group for yeast phosphoglycerate kinase reaction with Woodward's reagent K, J. Biol. Chem. 249 (1974) 5452–5457.
[15] T. Kiss, A. Erdei, L. Kiss, Investigation of the active site of the extracellular ss-D-xylosidase from *Aspergillus carbonarius*, Arch. Biochem. Biophys. 399 (2002) 188–194.
[16] A.A. Komissarov, D.V. Romanova, V.G. Debabov, Complete inactivation of *Escherichia coli* uridine phosphorylase by modification of Asp5 with Woodward's reagent K, J. Biol. Chem. 270 (1995) 10050–10055.
[17] K. Llamas, M. Owens, R.L. Blakeley, B. Zerner, N-Ethyl-5-phenylisoxazolium 3′-sulfonate (Woodward's Reagent K) as a reagent for nucleophilic side chains of proteins, Journal of the American Chemical Society 108 (1986) 5543–5548.
[18] P. Paoli, T. Fiaschi, P. Cirri, G. Camici, G. Manao, G. Cappugi, G. Raugei, G. Moneti, G. Ramponi, Mechanism of acylphosphatase inactivation by Woodward's reagent K, Biochem. J. 328 (1997) 855–861.
[19] P. Petra, Modification of carboxyl groups in bovine carboxypeptidase A. I. Inactivation of the enzyme by N-ethyl-5-phenylisoxazolium-3′-sulfonate (Woodward's reagent K), Biochemistry 10 (1971) 3163–3170.
[20] P. Petra, H. Neurath, Modification of carboxyl groups in bovine carboxypeptidase A. II. Chemical identification of a functional glutamic acid residue and other reactive groups, Biochemistry 10 (1971) 3171–3177.
[21] U. Sinha, J.M. Brewer, A spectrophotometric method for quantitation of carboxyl group modification of proteins using Woodward's Reagent K, Anal. Biochem. 151 (1985) 327–333.
[22] W. Vangrysperre, H. Kersters-Hilderson, M. Callens, C.K. De Bruyne, Reaction of Woodward's reagent K with D-xylose isomerases. Modification of an active site carboxylate residue, Biochem. J. 260 (1989) 163–169.
[23] C.W.G. VanGelder, W.H. Flurkey, H.J. Wichers, Sequence and structural features of plant and fungal tyrosinases, Phytochemistry 45 (1997) 1309–1323.
[24] A. Mohammadi, A.B. Moghaddam, R. Dinarvand, S. Rezaei-Zarchi, Direct electron transfer of polyphenol oxidase on carbon nanotube surfaces: application in biosensing, International Journal of Electrochemistry Science 4 (2009) 895–905.
[25] D.M. Sun, C.X. Cai, W. Xing, T.H. Lu, Immobilization and direct electrochemistry of copper-containing enzymes on active carbon, Chinese Science Bulletin 49 (23) (2004) 2452–2454.
[26] A.I. Yaropolov, A.N. Kharybin, J. Emneus, G. MarkoVarga, L. Gorton, Electrochemical properties of some copper-containing oxidases, Bioelectrochemistry and Bioenergetics 40 (1996) 49–57.
[27] B.X. Ye, X.Y. Zhou, Direct electrochemical redox of tyrosinase at silver electrodes, Talanta 44 (1997) 831–836.
[28] H. Zhou, L. Liu, K. Yin, S.L. Liu, G.X. Li, Electrochemical investigation on the catalytic ability of tyrosinase with the effect of nano titanium dioxide, Electrochemistry Communications 8 (2006) 1168–1172.
[29] N. Gheibi, A.A. Saboury, K. Haghbeen, A.A. Moosavi-Movahedi, Activity and structural changes of mushroom tyrosinase induced by n-alkyl sulfates, Colloids and Surfaces B: Biointerfaces 45 (2005) 104–107.
[30] P.H. Chen, R.L. McCreery, Control of electron transfer kinetics at glassy carbon electrodes by specific surface modification, Anal. Chem. 68 (1996) 3958–3965.
[31] G.E. Cabaniss, A.A. Diamantis, W.R. Murphy, R.W. L. Jr., T.J. Meyer, Electrocatalysis of proton-coupled electron-transfer reactions at glassy carbon electrodes, J. Am. Chem. Soc. 107 (1985) 1845–1853.
[32] G.B. Maralihalli, A.S. Bhagwat, Modification of maize phosphoenolpyruvate carboxylase by Woodward's reagent-K, J. Protein Chem. 12 (1993) 451–457.
[33] P. Tomme, M. Claeyssens, Identification of the functional important carboxyl group in cellobiohydrolase I from *Trichoderma reesei*: a chemical modification study, FEBS Lett. 243 (1989) 239–243.
[34] P. Tomme, J. Vanbeeumen, M. Claeyssens, Modification of catalytically important carboxy residues in endoglucanase-D from *Clostridium thermocellum*, Biochem. J. 285 (1992) 319–324.
[35] L. Stryer, The interaction of a naphthalene dye with apomyoglobin and apohemoglobin. A fluorescent probe of non-polar binding sites, J. Mol. Biol. 13 (1965) 482–495.
[36] C. SHI, Y. DAI, B. XIA, X. XU, Y. XIE, Q. LIU, The purification and spectral properties of polyphenol oxidase I from *Nicotiana tabacum*, Plant Molecular Biology Reporter 19 (2001) 381a-h.
[37] F.A. Armstrong, Probing Metalloproteins by Voltammetry, Structure and Bonding 72 (1990) 137–230.
[38] F.A. Armstrong, P.N. Cox, H.A.O. Hill, V.J. Lowe, B.N. Oliver, Metal ions and complexes as modulators of protein-interfacial electron transport at graphite electrodes, J. Electroanalytical Chemistry 217 (1987) 331–366.
[39] F.A. Armstrong, H.A.O. Hill, N.J. Walton, Direct electrochemistry of redox proteins, Acc. Chem. Res. 21 (1988) 407–413.
[40] N. Makino, P. McMahill, H.S. Mason, The oxidation state of copper in resting tyrosinase, J. Biol. Chem. 249 (1974) 6062–6066.
[41] J. Hong, A.A. Moosavi-Movahedi, H. Ghourchian, A.M. Rad, S. Rezaei-Zarchi, Direct electron transfer of horseradish peroxidase on Nafion-cysteine modified gold electrode, Electrochimica Acta 52 (2007) 6261–6267.

[42] R.W. Murray, A.J. Bard, Electroanalytical Chemistry, in, Marcel Dekker, New York, 1984 pp. 191–368.
[43] E. Laviron, The use of linear potential sweep voltammetry and of a.c. voltammetry for the study of the surface electrochemical reaction of strongly adsorbed systems and of redox modified electrodes, Journal of Electroanalytical Chemistry and Interfacial Electrochemistry 100 (1979) 263–270.
[44] A.J. Bard, L.R. Faulkner, Electrochemical Methods, in, Wiley, New York, 1980.
[45] E.I. Solomon, U.M. Sundaram, T.E. Machonkin, Multicopper oxidases and oxygenases, Chem. Rev. 96 (1996) 2563–2605.
[46] W.Q. Sun, G.F. Payne, M.S.G.L. Moas, J.H. Chu, K.K. Wallace, Tyrosinase reaction chitosan adsorption for removing phenols from waste-water, Biotechnology Progress 8 (1992) 179–186.